

Bifurcation length in the numerical simulation of the modulation instability

Agissilaos G. Athanassoulis and Irene Kyza

Department of Mathematics, University of Dundee

Monday 27th March, 2023

Abstract

The modulation instability (MI) is a well known feature of the focusing nonlinear Schrödinger equation (NLS), namely that plane wave solutions on the real line are linearly unstable. Simulations of the MI typically use a large computational domain of length L equipped with periodic boundary conditions. We show for the first time that for L smaller than a bifurcation length L_c the MI is completely suppressed in the periodized problem, and the abrupt bifurcation is also demonstrated numerically. Moreover, when the NLS is used to model water waves with typical wavelength λ_0 , the bifurcation lengthscale is $L_c = O(\lambda_0^2)$. Not accounting for that is artificially removing MI-related events in simulations.

Keywords: Nonlinear Schrödinger equation, Modulation instability, bifurcation, scientific computing

1 Introduction

The modulation instability (MI) is a fundamental feature of nonlinear waves. It has been re-discovered several times [18], and inspired a broad range of studies in physics, mathematics and beyond. However, a fundamental aspect regarding the numerical simulation of the MI is not clearly understood. The numerical solution of the NLS on the real line involves two key approximations: first the original problem is localized in space, i.e. substituted with the same equation on a bounded computational domain. Typically periodic boundary conditions are used, for two reasons: they preserve the translation invariant physics of the problem, and allow for solutions that don't decay at infinity, like perturbed

	$N = 0.98$	$N = 1.3$	$N = 3$	$N = 10$
$j = 1$	0.0359	2.59	3.08	3.03
$j = 2$	0.0393	2.59	3.09	3.03
$j = 3$	0.149	2.65	3.17	3.12
$j = 4$	0.25	2.69	3.22	3.18
$j = 5$	0.03	2.57	3.05	2.96

Table 1: Maximum value of the inhomogeneity $\max_{x,t} |\delta(x,t)|$ for $x \in [-L/2, L/2]$ and $t \in [0, 10]$, with $L = NL_c$ (cf. equation (16)) and initial condition $\delta_j(x, 0)$ (cf. equation (18)). See Section 5 for more details on the computation.

plane waves which are relevant for the MI. Secondly, the periodized problem is discretized, and solved in the computer. Traditional Numerical Analysis studies how well the solution of a discretized problem approximates the solution of its continuous counterpart. However, the continuous counterpart is the periodized problem, not the original one on the real line. In this paper we show that there exists a critical length L_c , depending on the original equation, so that periodizing on an interval shorter than L_c abruptly stabilizes the MI. That is, for the NLS on a short enough torus, plane wave solutions are linearly stable. Striking examples of that can be seen in Table 1 and in Figures 1, 2, 3.

Thus, no matter how sophisticated and accurate the discretization, the overall dynamics present in a simulation may be radically different from the intended problem on the real line because of periodization on a too short interval. For weaker nonlinearities the critical lengthscale becomes longer, and combined with the lack of awareness of the bifurcation it is possible that this artificial stabilization

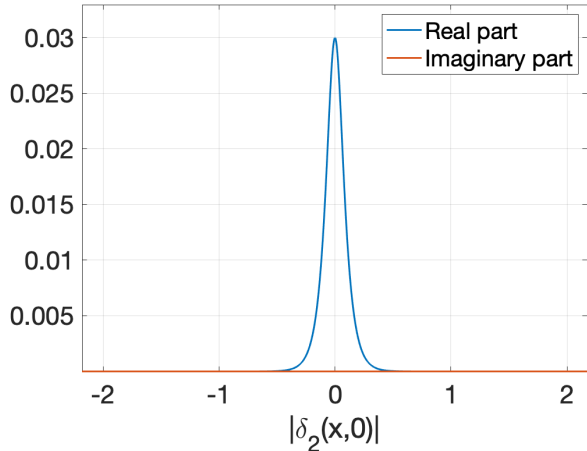


Figure 1: The initial inhomogeneity $\delta_2(x, 0)$ (cf. equation (17)) periodized on a domain of length $0.98L_c$. The initial inhomogeneity is well resolved, both in terms of number of points used and in terms of the extent of its support. Compare however with Figures 2, 3.

may be affecting state of the art simulations. We focus on water waves, where the problem is intrinsically weakly nonlinear (thus the bifurcation length quite large). This issue becomes increasingly important as numerical solutions are more and more heavily used to shed light to complex nonlinear wave problems – and most of these numerical solutions in fact discretize a periodized version of the NLS.

It should further be noted that the bifurcation lengthscale does not depend on the initial inhomogeneity. Even if the initial inhomogeneity is well contained in the computational domain, and a sufficiently fine computational mesh is used, this is no guarantee that the results approximate the solution of the corresponding problem on the real line – not even before the numerical solution reaches the boundary of the computational domain.

In Section 2 we discuss papers that are related with the existence of the bifurcation lengthscale L_c . We also discuss the ramifications for MI in water waves more broadly. In Section 3 we summarize the derivation of the classical MI for the NLS for completeness and clarity. In Section 4 we proceed to perform an analogous linear stability analysis for the periodized NLS. In Section 5 we use numerical simulation to explore the fully nonlinear behaviour of the problem. For the classical MI, our finding is that any computation aiming to simulate full space should use a computational domain at the very least

3 bifurcation lengthscales L_c long, and preferably $10L_c$ or more. In Section 6 we summarize the findings and compute the scaling of L_c for water waves problems.

2 State of the art

The complete suppression of the MI is a striking phenomenon, and its impact shows up indirectly in several works. In [9] the role of lengthscales in the stability of complex wavefields was investigated. Reduced dynamics for a wavetrain of characteristic length L were derived with implicit boundary conditions of linear dynamics away from the wavetrain. It was found that shorter lengthscales are fundamentally more stable, and would require unrealistically large-amplitude waves to be substantially amplified. In some cases, even complete stabilization for lengthscales shorter than a critical length was found. Analogous results were found in 2D in [17].

In the experimental paper [10] a wavelength $\lambda_0 = 3.5m$ is reported, and the tank is $74.5\lambda_0$ long (excluding the sloping part). Rogue waves with well-defined profiles are recovered. The same profiles were recovered in [11, 3] with two different sets of methods.

The onset of MI is also considered for more general wavefields – not only plane waves. It was shown in [1] that, for gaussian sea states with known power spectrum, an instability condition based on the shape of the spectrum can be derived. This instability condition and the onset of generalized MI when power spectra become narrow enough has been demonstrated e.g. in [15, 13, 16, 2, 4]. Numerical investigation of this predicted sudden onset of MI in realistic sea states has been complicated, as it involves many physical and numerical parameters, one of which is the size L of the computational domain. In [15] $L = 100\lambda_0$ was used. In [16] it is reported in Appendix A that after several attempts a lengthscale that works out to $L = 15\sqrt{2}L_c$ was found to be sufficient (along with a length of $\sqrt{2}L_c$ for the distance in the two-space correlation). More recently, in [4] it was found that L as large as $L = 126\lambda_0$ was required before the onset of the generalized MI could be observed.

On the other hand, there are many papers using computational domains of 10 – 20 wavelengths λ_0 , with some explicitly reporting that linear effects dominate the MI in their simulations, or that the

onset of the MI is not found. Indeed, “several wavelengths λ_0 ” is the default for many in the water waves community, since λ_0 is generally thought to be the fundamental lengthscale. However, the bifurcation length is $L_c = O(\lambda_0^2)$ as computed in detail in Section 6. Since the interesting wavelengths λ_0 are *in the hundreds of meters*, this explains e.g. the 70–130 wavelengths that were found to be required for the MI to manifest in the various studies mentioned here.

Beyond works looking specifically at the MI, there is now huge activity on extreme events and rogue waves. *The widespread use of the 10 – 20 λ_0 rule of thumb makes it entirely possible that many numerical experiments systematically underestimate MI-related events, because they are using computational domains that artificially stabilizes the MI.*

This work provides for the first time a systematic justification of the lengthscales required to simulate the classical MI, and a starting point for calibrating the numerical simulation of more general problems. Furthermore, this approach can be developed and applied to crossing seas, generalized MI and other more complex problems to quantify precisely the lengthscales required there.

3 Stability analysis on the real line and universality of the MI

Consider the NLS

$$i\partial_t u + p\Delta u + q|u|^2 u = 0 \quad (1)$$

for a wavefunction $u = u(x, t)$ on $x \in \mathbb{R}$ and $t \in [0, T]$, with boundary conditions of $\sup_{x \in \mathbb{R}} |u(x, t)| < \infty$ for all $t \in [0, T]$. These boundary conditions in particular allow for plane waves. The NLS is known to be well-posed in Zhidkov spaces [12, 19] (essentially spaces of smooth, globally bounded functions); this is the natural framework for this discussion. Also, since we are dealing with the focusing NLS, we will assume without loss of generality that $p, q > 0$.

The NLS (1) admits the exact solution

$$w(x, t) := Ae^{iqA^2 t}, \quad (2)$$

which is the simplest plane wave solution with amplitude $A > 0$. To study the stability of this plane wave solution one can consider whether small perturbations grow. This leads to the perturbed initial

value problem

$$\begin{aligned} i\partial_t u + p\Delta u + q|u|^2 u &= 0, \\ u(x, 0) &= A(1 + \delta_0(x)) \end{aligned} \quad (3)$$

for $x \in \mathbb{R}$ and $t \in [0, T]$ and some initial perturbation $\delta_0(x)$ which is small in an appropriate sense, $\delta_0 = o(1)$. Using the substitution

$$u(x, t) = Ae^{iqA^2 t}(1 + \delta(x, t)) \quad (4)$$

one readily computes that problem (3) is equivalent to

$$\begin{aligned} i\delta_t + p\Delta\delta + qA^2(\delta + \bar{\delta}) + \\ + qA^2(\delta + \bar{\delta})\delta + qA^2|\delta|^2(1 + \delta), \\ \delta(x, 0) = \delta_0(x). \end{aligned} \quad (5)$$

Dropping higher order terms, we obtain the linearized problem for the perturbation, namely

$$i\delta_t + p\Delta\delta + qA^2(\delta + \bar{\delta}), \quad \delta(x, 0) = \delta_0(x). \quad (6)$$

By expanding equation (6) into its real and imaginary parts, and denoting

$$\delta(x, t) = \alpha(x, t) + i\beta(x, t), \quad (7)$$

we eventually obtain the system

$$\begin{aligned} \partial_{tt}\beta + (p^2\Delta\Delta + 2pqA^2\Delta)\beta &= 0, \\ \partial_t\alpha + p\Delta\beta &= 0. \end{aligned} \quad (8)$$

This now can be solved explicitly with separation of variables, leading to the construction of the modes

$$\begin{aligned} \beta_\zeta(x, t) &= e^{i[\zeta x + \omega(\zeta)t]} + c.c., \quad \zeta \in \mathbb{R}, \\ \omega^2(\zeta) &= \zeta^2[p^2\zeta^2 - 2pqA^2]. \end{aligned} \quad (9)$$

(Here c.c. stands for complex conjugate.) More general solutions can be formed by superpositions of these modes, $\beta(x, t) = \int P(\zeta)\beta_\zeta(x, t)d\zeta$. The instability is due to the fact that,

$$|\zeta| < A\sqrt{\frac{2q}{p}} \implies \omega(\zeta) = \pm i|\omega(\zeta)| \quad (10)$$

and thus the corresponding modes $\beta_\zeta(x, t)$ of equation (9) contain an exponentially growing component. Therefore the solution δ of the linearized equation (6) generally grows exponentially in time, i.e. the plane wave solution of the NLS is linearly unstable. Moreover the unstable wavenumbers and their rate of growth follow from this analysis.

In this problem there are three parameters, p, q, A . However by rescaling the problem according to $\tau = qA^2 t$, $\chi = A\sqrt{\frac{q}{p}}x$, $U(\chi, \tau) = \frac{1}{A}u(x, t)$, the equation is mapped to the “canonical” NLS $i\partial_\tau U + \partial_{\chi\chi}U + |U|^2U = 0$, which has the plane wave solution $W(\chi, \tau) = e^{i\tau}$. That is, the exact values of p, q, A don't play an important role and the nature of the modulation instability is the same for any $p, q, A > 0$. This widely understood universality of the MI may have contributed to an implicit expectation that the periodized problem enjoys similar properties.

4 Stability analysis on the circle

Now let us consider the NLS equation (1) for $x \in [-\frac{L}{2}, \frac{L}{2}]$,

$$\begin{aligned} i\partial_t u + p\Delta u + q|u|^2 u &= 0, \\ x \in [-\frac{L}{2}, \frac{L}{2}], t \in [0, T], \end{aligned} \quad (11)$$

equipped with periodic boundary conditions,

$$\left\{ \begin{array}{l} u(-\frac{L}{2}, t) = u(\frac{L}{2}, t), \\ \partial_x u(-\frac{L}{2}, t) = \partial_x u(\frac{L}{2}, t), \end{array} \right\} \quad \forall t \in [0, T]. \quad (12)$$

The steps described above in equations (1)-(8) were carried out with boundary conditions of boundedness at infinity; however, one readily checks that each step is equally valid with the periodic boundary conditions on $[-L/2, L/2]$. Indeed, the plane wave is still a solution, the algebra leading to (5) is the same, and finally the linearization and separation of real and imaginary parts are the same. So now we have to solve the problem

$$\begin{aligned} \partial_{tt}\beta + (p^2\Delta\Delta + 2pqA^2\Delta)\beta &= 0, \\ \beta(-\frac{L}{2}, t) &= \beta(\frac{L}{2}, t), \\ \partial_x\beta(-\frac{L}{2}, t) &= \partial_x\beta(\frac{L}{2}, t). \end{aligned} \quad (13)$$

This is the first time that the parameter L really comes into play, and separation of variables now leads to the *discrete modes*

$$\begin{aligned} \beta_n(x, t) &= e^{2\pi i(\frac{nx}{L} + \omega_n t)} + c.c., \\ (2\pi\omega_n)^2 &= (\frac{2\pi n}{L})^2 [p^2(\frac{2\pi n}{L})^2 - 2pqA^2]. \end{aligned} \quad (14)$$

While this is analogous to equation (9), there is a very important difference: *depending on the values of p, q, A, L , there may not be even one unstable mode*. Indeed, $\omega_0 = 0$ and for any $0 \neq n \in \mathbb{Z}$ we have

$$\omega_n^2 < 0 \iff L > \frac{2\pi|n|}{A} \sqrt{\frac{p}{2q}}. \quad (15)$$

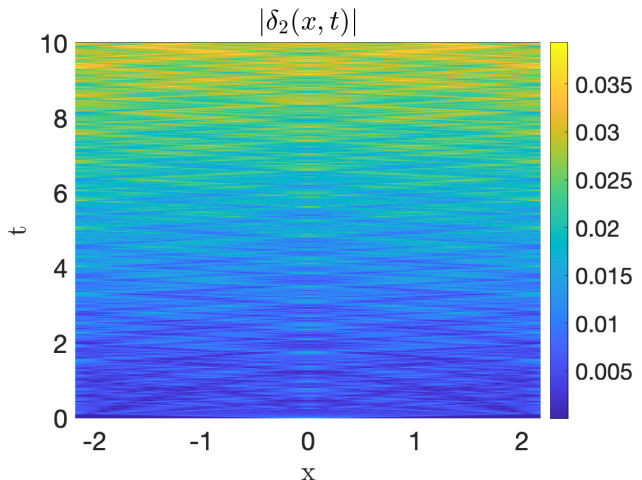


Figure 2: Space-time plot of $|\delta_2|$ when propagated on $0.98L_c$.

That is, the computational domain L has to be larger than

$$L_c := \frac{2\pi\sqrt{p}}{A\sqrt{2q}} \quad (16)$$

otherwise the MI is *completely suppressed*. We could say that the wavenumbers $\zeta \in (0, \zeta^*)$ are still unstable for $\zeta^* = A\sqrt{2q/p}$ just as in the real line. Indeed, any discrete wavenumbers $2\pi n/L > 0$ falling in $(0, \zeta^*)$ would be unstable – but the difference on the torus is that now a smallest positive wavenumber $2\pi/L$ exists. Thus if $2\pi/L > \zeta^*$, there are no unstable modes in the problem – something that was impossible on the real line. (The symmetric argument holds for negative wavenumbers.) So the numerical value of L_c is unsurprisingly $2\pi/\zeta^*$, but the change in the nature of MI from \mathbb{R} to the torus (i.e. the capacity for complete elimination of the instability) is due to the discretization of the spectrum.

Observe moreover that the lengthscale L_c does not depend on the initial inhomogeneity $\delta_0(x)$, and becomes larger when the nonlinearity becomes weaker (i.e. when $q, A > 0$ decrease).

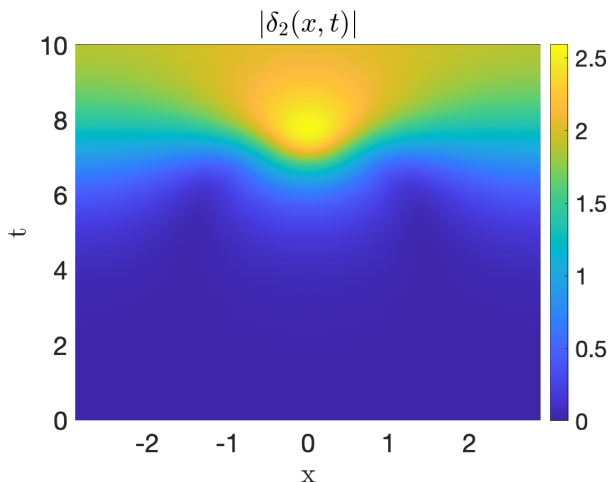


Figure 3: Space-time plot of $|\delta_2|$ when propagated on $1.3L_c$.

5 Numerical investigation in the number of unstable modes

In what follows we present numerical solutions of the problem

$$\begin{aligned} i\partial_t u + p\Delta u + q|u|^2 u &= 0, \\ u(-\frac{L}{2}, t) &= u(\frac{L}{2}, t), \quad \partial_x u(-\frac{L}{2}, t) = \partial_x u(\frac{L}{2}, t), \\ u(x, 0) &= A(1 + \delta_j(x)) \end{aligned} \quad (17)$$

for the initial inhomogeneities

$$\begin{aligned} \delta_1(x) &= A(1 + 0.03 \cdot \text{sech}(15x) \cos(5x)), \\ \delta_2(x) &= A(1 + 0.03 \cdot \text{sech}(15x)), \\ \delta_3(x) &= A(1 + 0.03 \cdot e^{-3x^2}), \\ \delta_4(x) &= A(1 + 0.03 \cdot e^{-x^4}), \\ \delta_5(x) &= A(1 + 0.06 \cdot x \cdot e^{-x^4}), \\ \delta_6(x) &= A(1 + 0.03 \cdot \text{sech}(0.33x)), \end{aligned} \quad (18)$$

and $p = q = A = 1$. The bifurcation length in this case is $L_c \approx 4.45$; the solutions will be computed for $L = 0.98L_c$, $L = 1.3L_c$, $L = 3L_c$ and $L = 10L_c$. The computation time is $t \in [0, 10]$. The numerical scheme used is a relaxation in time with mass and energy conservation [5, 6], with second-order finite differences in space. The full code is included in the supplement. The inhomogeneity $\delta(x, t)$ for $t \in [0, 10]$ is defined as

$$\delta(x, t) := (u(x, t) - Ae^{iqA^2t}) \frac{1}{A} e^{-iqA^2t} \quad (19)$$

consistently with equation (4).

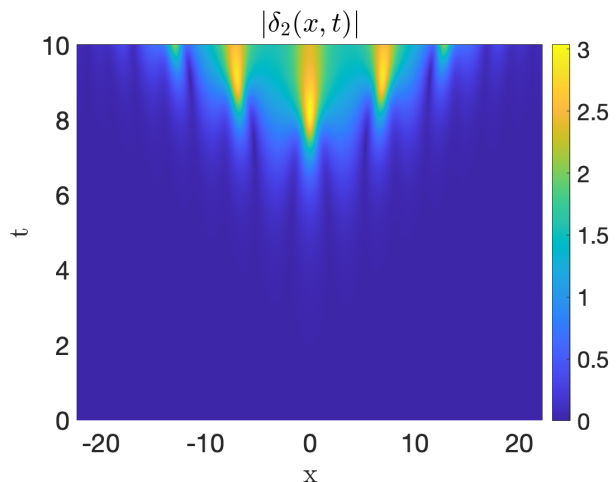


Figure 4: Space-time plot of $|\delta_2|$ for $L = 10L_c$.

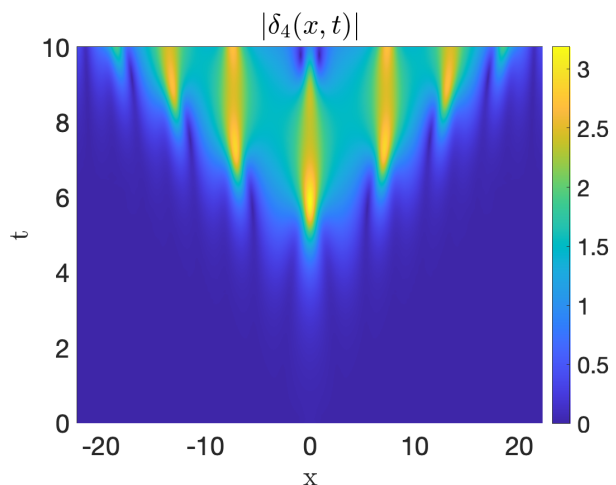


Figure 5: Space-time plot of $|\delta_4|$ for $L = 10L_c$.

The inhomogeneities δ_1 and δ_2 are localized sech bumps, and are quite similar to each other. δ_3 and δ_4 are also bumps with different profiles, and δ_5 is a localised wave. δ_6 is a version of δ_2 dilated to have 45 times wider support, longer than L_c . Its support is larger than L_c , so it is not useful to demonstrate the bifurcation – rather it is included to highlight the coherent structure that emerges on long enough domains (more details below).

In Table 1 the maximum moduli of the inhomogeneities are recorded when propagated on intervals of different lengths. There is a clear confirmation of the abrupt bifurcation predicted in Section 4, namely an abrupt change in behaviour from $L = 0.98L_c$ to $L = 1.3L_c$.

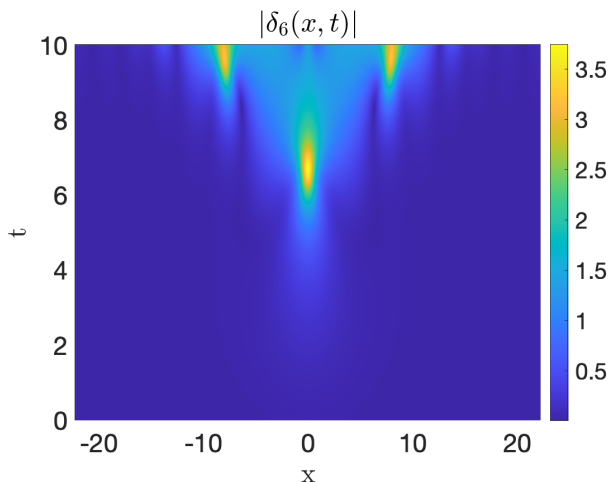


Figure 6: Space-time plot of $|\delta_6|$ for $L = 10L_c$.

On the larger intervals $L = 3L_c$, $L = 10L_c$, coherent structures emerge. These are the sign that the MI has been resolved in a manner qualitatively similar to what would happen on the real line (that is, until the structures reach close to the boundary of the computational domain) [8, 7]. These structures all involve localised maxima supported on neighbourhoods of size roughly L_c each, arranged homogeneously in a space-time cone. Moreover, the simulation of δ_6 shows that these blobs can also result from the inhomogeneity *shrinking*, not only expanding. All initial inhomogeneities examined here, when propagated on a large enough interval, give rise to qualitatively similar coherent structures, clearly seen in Figures 4, 5 and 6. To clearly see even one local maximum, we observe that a computational domain of at least $3L_c$ is required. This seems to allow for a qualitatively correct view of the tip of the cone for a short time (of course the solution no longer corresponds to the real line when the cone comes to close to the boundary).

When the length of the domain becomes $L < L_c$, we don't merely see a periodised or slightly off version of the cone, but something completely different: the amplification is small or non-existent and there is no spatial pattern at all, cf. Figures 2, 7. Indeed, for all initial data, when $L = 0.98L_c$, the inhomogeneity initially disperses rapidly and then slowly grows in homogeneous way over the whole computational domain.

The question of a universal pattern in the MI [8, 7] is relevant to universal profiles of Rogue waves

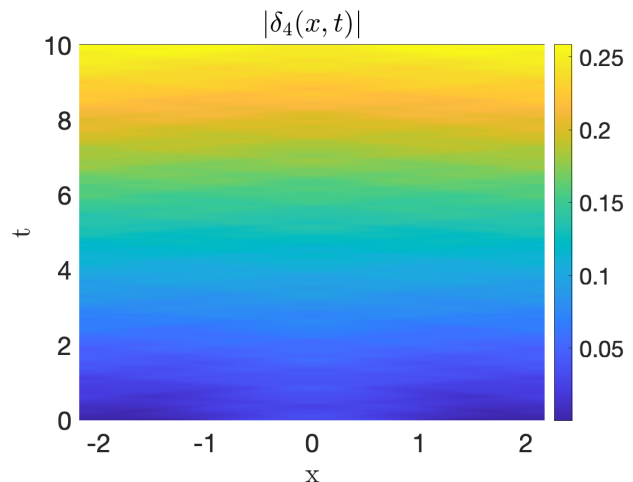


Figure 7: Space-time plot of $|\delta_4|$ for $L = 0.98L_c$.

[11, 10] although that discussion is beyond the scope of this paper. In any case, the numerical results confirm that the coherent structures emerging in the nonlinear phase of the MI exhibit the lengthscale L_c independently of the initial inhomogeneity and its width. Thus, *a computational domain of at least a few L_c is crucial when simulations of the MI are carried out with periodic boundary conditions*. In particular, taking a domain much larger than the effective support of the initial inhomogeneity is no guarantee that the numerical solution does look like what would happen on the real line, not even before the solution reaches the boundary.

6 Conclusions

The finding here is that periodizing the NLS can completely remove the MI, when an interval shorter than the bifurcation length L_c is used. Moreover, this can present as a very abrupt bifurcation, where a small change in the length of the domain can lead to a huge difference in the dynamics.

For water waves with typical wavenumber k_0 (equivalently typical wavelength $\lambda_0 = 2\pi/k_0$), the coefficients are $p = \sqrt{g}/(8k_0^{3/2})$, $q = \sqrt{g}k_0^{5/2}/2$ [14] leading to

$$L_c = \frac{1}{4\pi\sqrt{2}} \frac{\lambda_0^2}{A}. \quad (20)$$

So for large wavelengths and weak nonlinearities, requiring a computational domain of many wavelengths is not surprising. Note that the waves that would be dangerous for ships in the ocean and carry

most of the surface wave energy have wavelengths in the hundreds of meters. Moreover, a spectrum that is barely narrow enough to trigger MI in the sense of [1], exhibits a weak MI – which would likely function like a small A in equation (20). The combination of these factors make a bifurcation length scale L_c in the hundreds of wavelengths likely. This should be accounted for in simulations of extreme events and rogue waves.

Acknowledgment. The authors would like to thank Prof. G. A. Athanassoulis, Prof. T. Sapsis, Dr. O. Gramstad and Dr. T. Tang for helpful discussions.

References

- [1] I. E. ALBER, *The Effects of Randomness on the Stability of Two-Dimensional Surface Wavetrains*, Proceedings of the Royal Society A: Mathematical, Physical and Engineering Sciences, 363 (1978), pp. 525–546.
- [2] A. ATHANASSOULIS, G. ATHANASSOULIS, M. PTASHNYK, AND T. SAPSIS, *Strong solutions for the Alber equation and stability of unidirectional wave spectra*, Kinetic and Related Models, 13 (2020), pp. 703–737.
- [3] A. ATHANASSOULIS, G. ATHANASSOULIS, AND T. SAPSIS, *Localized instabilities of the Wigner equation as a model for the emergence of Rogue Waves*, Journal of Ocean Engineering and Marine Energy, 3 (2017), pp. 353–372.
- [4] A. G. ATHANASSOULIS, *Phase Resolved Simulation of the Landau-Alber Stability Bifurcation*, Fluids, 8 (2023).
- [5] C. BESSE, *A relaxation scheme for the nonlinear Schrödinger equation*, SIAM Journal on Numerical Analysis, 42 (2004), pp. 934–952.
- [6] C. BESSE, S. DESCOMBES, G. DUJARDIN, AND I. LACROIX-VIOLET, *Energy-preserving methods for nonlinear Schrödinger equations*, IMA Journal of Numerical Analysis, 41 (2021), pp. 618–653.
- [7] G. BIONDINI, S. LI, D. MANTZAVINOS, AND S. TRILLO, *Universal behavior of modulationally unstable media*, (2017).
- [8] G. BIONDINI AND D. D. MANTZAVINOS, *Universal Nature of the Nonlinear Stage of Modulational Instability*, Physical Review Letters, 116 (2016), pp. 1–5.
- [9] W. COUSINS AND T. P. SAPSIS, *Unsteady evolution of localized unidirectional deep-water wave groups*, Physical Review E - Statistical, Nonlinear, and Soft Matter Physics, 91 (2015), pp. 1–5.
- [10] G. DEMATTEIS, T. GRAFKE, M. ONORATO, AND E. VANDEN-EIJNDEN, *Experimental Evidence of Hydrodynamic Instantons: The Universal Route to Rogue Waves*, Physical Review X, 9 (2019), p. 41057.
- [11] G. DEMATTEIS, T. GRAFKE, AND E. VANDEN-EIJNDEN, *Rogue Waves and Large Deviations in Deep Sea*, Proceedings of the National Academy of Sciences, (2018), p. 201710670.
- [12] C. GALLO, *Schrödinger group on Zhidkov spaces*, Advances in Differential Equations, 9 (2004), pp. 509–538.
- [13] O. GRAMSTAD, *Modulational Instability in JONSWAP Sea States Using the Alber Equation*, in ASME 2017 36th International Conference on Ocean, Offshore and Arctic Engineering, 2017.
- [14] C. C. MEI, M. STIASSNIE, AND D. K.-P. YUE, *Theory and Applications of Ocean Surface Waves*, vol. 23 of Advanced Series on Ocean Engineering, World Scientific, jul 2005.
- [15] M. ONORATO, A. OSBORNE, R. FEDELE, AND M. SERIO, *Landau damping and coherent structures in narrow-banded 1 + 1 deep water gravity waves*, Physical Review E, 67 (2003), p. 046305.
- [16] A. RIBAL, A. V. BABANIN, I. YOUNG, A. TOFFOLI, AND M. STIASSNIE, *Recurrent solutions of the Alber equation initialized by Joint North Sea Wave Project spectra*, Journal of Fluid Mechanics, 719 (2013), pp. 314–344.
- [17] T. TANG AND T. A. ADCOCK, *A reduced order model for space-time wave statistics using probabilistic decomposition-synthesis method*, Ocean Engineering, 259 (2022), p. 111860.

- [18] V. E. ZAKHAROV AND L. A. OSTROVSKY, *Modulation instability: The beginning*, Physica D: Nonlinear Phenomena, 238 (2009), pp. 540–548.
- [19] P. ZHIDKOV, *The Cauchy problem for the non-linear Schrödinger equation*, tech. rep., Joint Inst. for Nuclear Research No. JINR-R-5-87-373, 1987.